

Carrier transfer in the optical recombination of quantum dots

D. F. Cesar,^{*} M. D. Teodoro, V. Lopez-Richard, and G. E. Marques

Departamento de Física, Universidade Federal de São Carlos, 13.565-905 São Carlos, São Paulo, Brazil

E. Marega Jr.

Instituto de Física de São Carlos, Universidade de São Paulo, CP 369, 13560-970 São Carlos, SP, Brazil

V. G. Dorogan, Yu. I. Mazur, and G. J. Salamo

Department of Physics, University of Arkansas, 226 Physics Building, Fayetteville, Arkansas 72701, USA

(Received 8 March 2011; published 9 May 2011)

We report a study of dynamic effects detected in the time-resolved emission from quantum dot ensembles. Experimental procedures were developed to search for common behaviors found in quantum dot systems independently of their composition: three quantum dot samples were experimentally characterized. Systems with contrasting interdot coupling are compared and their sensitivity to the excitation energy is analyzed. Our experimental results are compared and contrasted with other results available in literature. The optical recombination time dependence on system parameters is derived and compared to the experimental findings. We discuss the effects of occupation of the ground state in both valence and conduction bands of semiconductor quantum dots in the dynamics of the system relaxation as well as the nonlinear effects.

DOI: [10.1103/PhysRevB.83.195307](https://doi.org/10.1103/PhysRevB.83.195307)

PACS number(s): 73.21.La, 78.47.jd

I. INTRODUCTION

The interest in the carrier dynamics of semiconductor quantum dots (QDs) has been renewed since the control of energy relaxation and correlations in collective QD emission have potential implications in proposals for optoelectronic devices. The characterization of time resolved emissions from QDs has emerged as a crucial tool that enables the understanding of combined processes of recombination, relaxation, and interaction between carriers.¹⁻⁴ Despite the broad range of studies, some questions remain open: Why under certain conditions has a sharp increase of the radiative decay times been experimentally confirmed?⁵ How may nonlinear mechanisms emerge from the imbalanced occupancy of electron and hole states along with optical and electronic coupling and what would be their effect on the recombination process?⁶⁻⁸ The local charge imbalance in QDs has implications in the magneto-photoluminescence (PL) of QDs as reported in Ref. 9: could this effect be experimentally confirmed in time resolved emissions?

Several mechanisms in the relaxation process may simultaneously take part and the elucidation of predominant effects becomes a difficult task where neglecting the statistics underneath might underestimate the influence of nonequilibrium conditions. This will be highlighted in this work along with the role of phonons in the process of interdot charge transfer.¹⁰ The local carrier imbalance is also determined by the asymmetric interdot transfer of electrons or holes assisted by phonons. Thus this work correlates all these effects into a systematic analysis pointing out common properties found in QD systems of different nature. For that, along with our own experimental samples (labeled as samples 1, 2, 3) we have also included results reported in published works of various authors.

The structures corresponding to samples 1, 2, and 3 are formed by In_{0.4}Ga_{0.6}As/GaAs QDs grown on semi-insulating GaAs (001) substrates by molecular-beam epitaxy. After removing the oxidized layer from the substrate surface, a

0.3- μ m GaAs buffer layer was grown at 580 °C. Then, the temperature was reduced to 540 °C for the growth. Sample 1 is a 15-period (2.5 nm) In_{0.4}Ga_{0.6}As/(60 monolayers) GaAs multilayer structure grown using As₄ background. Samples 2 and 3 are single (2.5 nm) In_{0.4}Ga_{0.6}As QDs layer capped with 50 nm of GaAs. In Sample 2, an As₄ background was used to form the QDs structures unlike sample 3, where As₂ was used. The influence of the As background on QD formation has been described in Ref. 11.

II. RESULTS

In Fig. 1(a), the decay times labeled sample 1 were extracted from the time-resolved PL from dense In_{0.4}Ga_{0.6}As/GaAs QD chains described in Ref. 7. As a reference, we have also included the PL emission spectrum from this sample. The data labeled as experiments 2 and 3 were taken from Ref. 5: Experiment 2 corresponds to the emission from a reference sample of uncoupled InGaAs/GaAs QDs whereas experiment 3 comes from InGaAs/GaAs QD chains. In the case of Fig. 1(b), the data labeled as experiment 4 were extracted from Ref. 6 corresponding to the emission from a single layer of self-assembled CdSe/ZnSe QDs (the PL spectrum included in this panel was also taken from Ref. 6).

For low light intensities, the carrier interaction with radiation can be considered as a perturbation and the magnitude of the optical decay time can be calculated by using the standard Fermi “golden rule,”¹

$$\tau_0(\hbar\omega) = \frac{3 \hbar c m_0 c^2}{4 e^2} \frac{1}{n} \frac{\hbar}{| \langle F_e | F_h \rangle |^2 E_p \hbar \omega}, \quad (1)$$

where n is the refractive index in the material, E_p is the Kane energy, and $| \langle F_e | F_h \rangle |^2$ accounts for the overlapping between electron and hole wave functions. At first glance, the functional dependence of the decay time with the emission energy is rather simple ($\tau_0 \propto \frac{1}{\hbar\omega}$) and, in principle, monotonic

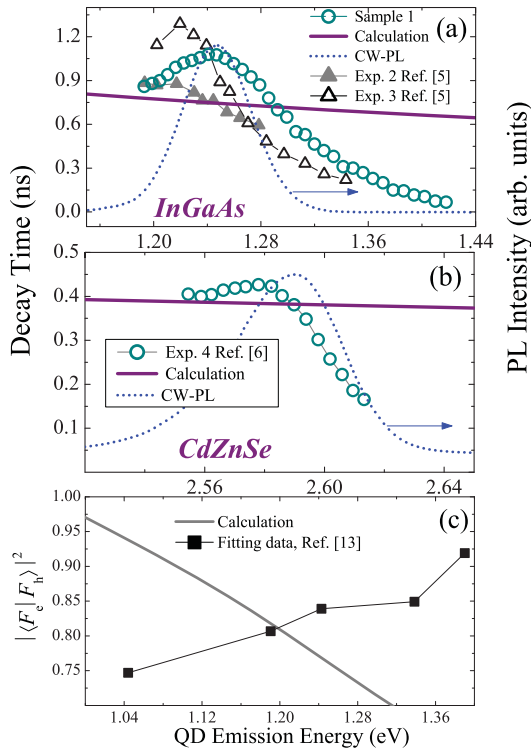


FIG. 1. (Color online) Decay time vs emission energy for different QD samples. (a) Various InGaAs/GaAs QD samples. (b) CdSe/ZnSe QD sample. The solid curves represent the calculation for a single QD model of Eq. (1). (c) $|\langle F_e|F_h\rangle|^2$ vs emission energy in a InGaAs/GaAs QD. Solid curve: theoretical calculation; squares: fitting data from Ref. 13.

as displayed in Figs. 1(a) and 1(b) as solid curves for InAs and CdSe QDs, respectively. However, experimental observations indicate that such a monotonic behavior is not accurately followed. The experimental decay times as a function of the emission energy of different QD samples have been compared to the result of Eq. (1) and displayed in Figs. 1(a) and 1(b) (a similar functional dependence can be also found in Ref. 12).

As we can see in Fig. 1(a), the calculation using Eq. (1), for which we considered $|\langle F_e|F_h\rangle|^2 = 1$, gives a reasonable agreement with the values of experiment 2, corresponding to the reference sample of uncoupled QDs. For the rest of the experimental data the disagreement is evident for both InGaAs and CdSe QDs that display analogous functional behavior. Thus as pointed out in Ref. 6, QD chain samples do not behave like individual independent objects as long as they form an ensemble, and we focused our discussion on these collective effects. We can divide this study into two main issues: for low energies the experimental decay time lies above the predicted value of Eq. (1) and shows a nonmonotonic behavior with the energy. Yet for higher energies the decay time drops below the reference values. In Ref. 13, this sharp decrease is ascribed to an increase with energy of the overlapping between the envelope functions of electrons and holes. In this reference, $|\langle F_e|F_h\rangle|^2$ was used as a free fitting parameter and displayed as square symbols in Fig. 1(c). However, the dependence of this overlapping factor on energy cannot account for the expected functional behavior of the decay time. In Fig. 1(c) we show the calculated dependence of the overlapping with energy: as

the QDs become smaller the overlapping decreases. Given the smaller electron mass with respect to the heavy holes, the effect of confinement is not symmetric and the penetration of electrons and holes wave function into the barriers is differently tuned with confinement. For low energies (bigger QDs) the electrons and holes are more localized inside the QD and they have a more pronounced overlapping. Yet for high energies (smaller QDs) a larger penetration of electron wave function into the barriers is achieved leading to a weaker overlapping. Thus we cannot ascribe the observed functional behavior of the decay time with the emission energy to the functional behavior of the overlapping integral. One must also note that the overlapping parameter has a maximum value $|\langle F_e|F_h\rangle|^2 = 1$ and cannot be responsible for the experimental decrease of the decay time below τ_0 for higher energies. The effect of geometry and strain will also have a direct impact in the optical response and affect, in particular, the electron-hole overlapping. A detailed analysis of the shape and strain fields in the QDs under consideration can be found in Ref. 14. It was found that the anisotropic geometry of the QD shape may lead to the hybridization of the valence-band ground state, which would subsequently affect the value of the optical transition matrix element. In turn, the strain field strength depends on QD array formation and interdot distance and affects the optical transition rate by tuning the separation between the coupled heavy and light hole subbands. The character of the valence-band ground state may be effectively tuned by relaxing the strain fields. This can be achieved by thermal annealing, as reported in Ref. 15.

For smaller dots, nonradiative relaxation channels are active inducing the reduction of the effective lifetime of the ground state:¹² An effective carrier transfer takes place between adjacent dots with different size leading to a cascadelike process of decay from the ground state of smaller dots to a neighbor excited states of bigger dots. This process is assisted by longitudinal optical (LO)-phonon emission in QD ensembles.¹⁰ It leads not only to the sharp decay time reduction for smaller QDs but also contributes to the imbalance between electron and hole occupancies in bigger QDs that will subsequently lead to the nonmonotonic behavior of the decay time observed in the experiments, as will be shown below.

To describe phonon effects on carrier decay time in QD chains we considered the Fröhlich interaction to calculate the ground-state lifetime, given

$$\frac{1}{\tau_p} = \frac{2\pi}{\hbar} \sum_q |\langle \psi_n | \mathcal{H}_{e\text{-phonon}}^{\text{LO}} | \psi_{n'} \rangle|^2 \rho_{\text{phonon}}, \quad (2)$$

where q is the phonon wave vector, $\mathcal{H}_{e\text{-phonon}}^{\text{LO}}$ is the electron-phonon interaction Hamiltonian, and ρ_{phonon} is the phonon density of states given by

$$\rho_{\text{phonon}} = \frac{1}{\pi} \frac{\Gamma_{\text{LO}}}{(\Delta E - \hbar\omega_{\text{LO}}) + \Gamma_{\text{LO}}^2}, \quad (3)$$

where $\hbar\omega_{\text{LO}}$ is the longitudinal-optical phonon energy and ΔE is the energy difference between $|\psi_{n'}\rangle$ and $|\psi_n\rangle$ states with the phonon width $\Gamma_{\text{LO}} = 0.0409$ meV.¹⁶

For stacked coupled QDs, we obtain

$$\frac{1}{\tau_p} = \frac{2\pi}{\hbar} \rho_{\text{phonon}} \frac{\sqrt{2}}{(2\pi)^2} \alpha (\hbar\Omega)^2 \mathcal{P}_{nn'}, \quad (4)$$

where α is the Fröhlich constant, $\hbar\Omega$ is the confinement energy related to the xy coordinates, which is given by $\hbar\Omega = \frac{4\hbar^2}{m^* D^2}$, D is the dimension responsible for the confinement, and m^* is the carrier effective mass. $\mathcal{P}_{nn'}$ is given by

$$\mathcal{P}_{nn'} = 2\pi \int_0^{+\infty} dq_z |I_{nn'}(q_z)|^2 \left\{ -e^{q_z^2/2} E_i \left(-\frac{q_z^2}{2} \right) \right\}, \quad (5)$$

where $I_{nn'}(q_z) = \int_{-\infty}^{+\infty} \psi_n e^{iq_z z} \psi_{n'} dz$. The Fröhlich constant α will suffer a renormalization in the QD and is given by¹⁷ $\alpha_{\text{dot}} = \alpha_{\text{bulk}} \frac{\epsilon'_{\text{bulk}}}{\epsilon'_{\text{dot}}} \sqrt{\frac{m_e^{\text{dot}}}{m_e^{\text{bulk}}}}$, where the bulk value corresponds to $\alpha_{\text{bulk}} = \frac{e}{\epsilon'_{\text{bulk}}} \sqrt{\frac{m_e}{2\hbar^3 \omega_{\text{LO}}}}$. Here ϵ'_{bulk} and ϵ'_{dot} are, respectively, given by $\frac{1}{\epsilon'_{\text{bulk}}} = \frac{1}{\epsilon_\infty} - \frac{1}{\epsilon_0}$ and $\frac{1}{\epsilon'_{\text{dot}}} = \frac{1-a/D}{\epsilon_\infty} - \frac{1}{\epsilon_0} + \frac{a}{D}$, where a is the separation between QDs.

Figure 2 shows the effect of QD coupling by LO phonons on the carrier life time for the resonant condition. The calculations were performed for InGaAs/GaAs QD chains considering both the bulk and QD Fröhlich constant. The effective interdot charge transfer assisted by phonon emission induces a reduction of the decay time in smaller dots given by $1/\tau_p + 1/\tau_0$. The probability of finding a configuration of smaller dots with an adjacent neighbor with a lower ground state separated in one LO phonon is rather high given the predominant appearance of QDs with energies near the PL maximum. An additional decrease of decay times is due to strain fields that lead to the effective reduction of barrier heights; this is more effective for electrons than for heavy holes. Thus, for higher energies, the reduction of the decay time below the reference values, $\tau_0(E)$, in Figs. 1(a) and 1(b) can be ascribed to the effective carrier escape through phonon emission. The decay time increases above $\tau_0(E)$ for lower energies and its nonmonotonic behavior is still to be discussed. By contrasting Figs. 2(a) and 2(b), asymmetric values of the lifetimes of electrons and holes

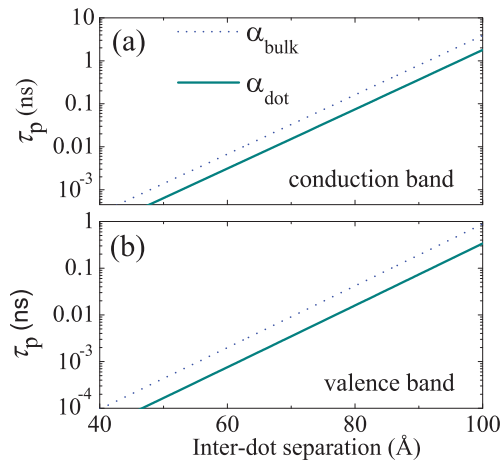


FIG. 2. (Color online) Phonon effects on carrier lifetime in quantum-dot chains as a function of QD separation (a) for electrons and (b) for heavy holes. Solid curves represent the calculation using α_{dot} , and dotted curves correspond to the value α_{bulk} .

appear. Such a difference will lead to a local and temporal imbalance between carriers in the process of recombination in larger QDs. In Ref. 18, a discussion can be found about the potential effect of interdot coupling in the experimentally extracted decay time of coupled QDs. Also in this case various samples were tested with different In content that would, in principle lead to variations of the electronic structure, however, it has been shown that the main effect that shapes the relaxation and recombination process is the interdot electronic coupling tuned by interdot distance.

Electrons and holes, in a system which is relaxing, can be found away from thermal equilibrium¹⁹ hence a local (and temporal) charge imbalance must be taken into account. This is an effect usually neglected when dealing with nonstationary conditions as stated in Ref. 2. By labeling the density of electrons in the conduction-band ground state as n_e and n_h in the valence band, a model that accounts for the charge fluctuations can be reduced to

$$\begin{aligned} \frac{dn_e^x}{dt} &= -\frac{n_e^x}{\tau_e^R}, & \frac{dn_e}{dt} &= \frac{n_e^x}{\tau_e^R} - \frac{n_e \cdot f_h(n_h)}{\tau_0}, \\ \frac{dn_h}{dt} &= \frac{n_h^x}{\tau_h^R} - \frac{n_h \cdot f_e(n_e)}{\tau_0}, & \frac{dn_h^x}{dt} &= -\frac{n_h^x}{\tau_h^R}, \end{aligned} \quad (6)$$

for $n_{e(h)} < 1$, with the occupation distribution given by

$$f_{h(e)}(n_{h(e)}) = \begin{cases} n_{h(e)}/2 & n_{h(e)} < 2 \\ 1 & n_{h(e)} \geq 2 \end{cases}.$$

In this case, we have considered the double degeneracy of the ground states in the absence of a magnetic field. The initial conditions will be $n_e(0) = n_h(0) = 0$, $n_e^x(0) = \delta N_e^{\text{max}}$, and $n_h^x(0) = \delta N_h^{\text{max}}$. In principle, due to neutrality, one could assume that $\delta N_h^{\text{max}} = \delta N_e^{\text{max}}$, however, charge imbalance may take place locally. The emission intensity due to optical recombination from the electron-hole pair ground state will be given by $I_{\text{PL}} = \frac{n_{e(h)} \cdot f_{h(e)}(n_{h(e)})}{\tau_0}$, for $n_{e(h)} < 1$. Note that the effective recombination time $\tau_{\text{eff}} = \tau_0 / f_{h(e)}$ varies throughout the whole process since, in general, $f_{h(e)} \leq 1$. Yet a limit value for the exponential decay time can be attained for long times that will be different from τ_0 .

In Fig. 3(a), the results of the calculations based on Eqs. (6) are shown as a function of the initial hole density for various values of the initial electron density. We can see that the net effect consists of an increasing decay time above τ_0 . In this way, different excitation regimes of each QD can lead to different values of the decay time. Note that for equal initial values of electrons and holes (balanced charges), the decay time sharply grows and attains a maximum.

In order to set a correlation between this effect and the emission energy we shall assume that the total number of initial carriers per dot (emitting photons with energy E), $\delta N^{\text{max}}(E)$, is proportional to the number of absorbed photons, N_{absorbed} : $\delta N^{\text{max}}(E) = N_{\text{absorbed}} / N_{\text{dots}}(E)$. In turn, the distribution of QDs by size results in the distribution of states by energy detected by the PL. Thus $N_{\text{dots}}(E)$ follows the Gaussian profile of the PL emission spectra as those shown in Figs. 1(a) and 1(b). This size (energy) distribution of QDs will determine the sequence of steps in the relaxation and asymmetric carrier transfer processes that will lead to charge imbalance between electrons and holes. Let us assume an imbalance between

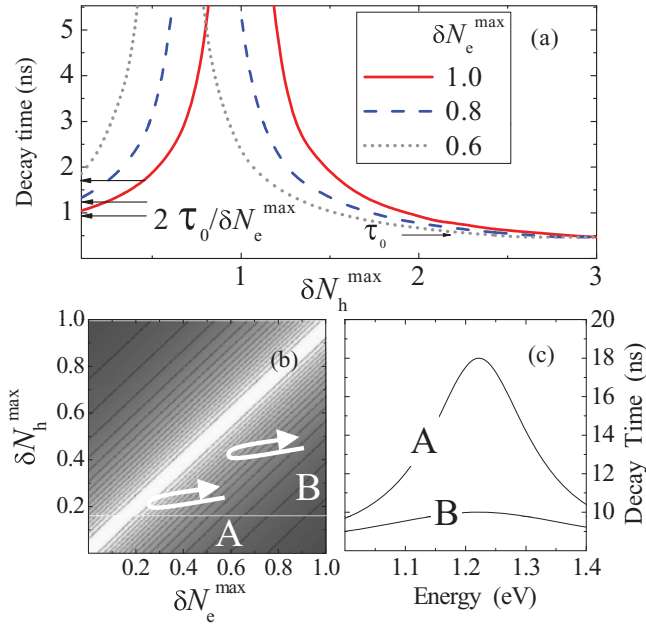


FIG. 3. (Color online) (a) Decay time calculated according Eq. (6). (b) Three-dimensional color scheme corresponds to the decay time as represented in panel (a). (c) Decay time as a function of energy for two hypothetical paths, A and B, as displayed in panel (b).

electrons and holes leading to the condition $\delta N_e^{\max}(E) > \delta N_h^{\max}(E)$. We can thus write $\delta N_e^{\max}(E) = \alpha \delta N_h^{\max}(E)$, with $\alpha < 1$. Then, given that the $N_e^{\max}(E) \propto N_{\text{absorbed}}/N_{\text{dots}}(E)$, the total number of initial carriers per dot, as the energy increases, follows paths analogous to those labeled A or B in Fig. 3(b). The corresponding decay time as a function of energy is shown in Fig. 3(c): a nonmonotonic behavior as observed in the experiments displayed in Figs. 1(a) and 1(b). Note that the system is highly sensitive to the initial conditions.

The dependence on initial excitation conditions was tested in two samples formed by $\text{In}_{0.4}\text{Ga}_{0.6}\text{As}$ QDs, both structurally described in Ref. 14: one with closely lying dots, sample 2, and another with them randomly separated, sample 3, as displayed at the top of Fig. 4. The QDs in sample 2 are mostly aligned along the $[1\bar{1}0]$ direction. The values of the decay time were extracted for three different excitation energies down to the near-resonance condition [Figs. 4(a)–4(c)].

For nonresonant excitation [Figs. 4(a) and 4(b)] the decay time is different for each given sample close to the region of PL maximum. Clearly, the carrier transfer from smaller to larger dots affects differently the charging condition of the predominant QDs that emit close to the position of the PL maximum. The asymmetric interdot carrier transfer that leads to the charge imbalance is more effective in sample 2 and weakened in sample 3. Thus in accordance with Fig. 3(a), the decay time in sample 2 should be smaller than in sample 3. As the excitation energy approaches the value of the PL maximum, the decay times of both samples become similar. In this case, the process of interdot transfer becomes less effective in sample 2 leading to the decay time increase close to the values obtained for sample 3.

In Fig. 4(d), we show the PL transients extracted at the energies T_1 , T_2 , and T_3 in panel (a). For T_1 , the nonradiative

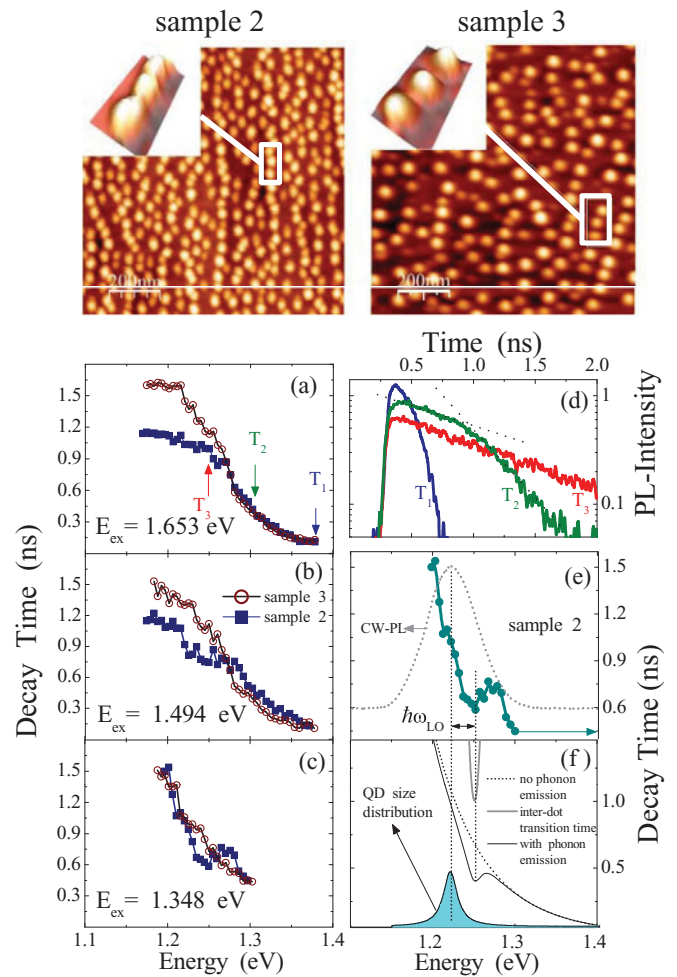


FIG. 4. (Color online) AFM images of QD samples 2 and 3 are displayed at the top. (a)–(c) Decay time vs emission energy for both samples at three values of the excitation energy. (d) PL transients at the emission energy values labeled T_1 , T_2 , and T_3 in panel (a). (e) Decay time of sample 2 under near-resonance excitation (PL spectrum has been added for reference). (f) Calculated values of the decay time during the interdot carrier transfer assisted by phonon emission.

charge escape from smaller QDs prevails, then for T_3 , the optical recombination appears to dominate on the long time, yet at the intermediary point T_2 , both processes shape the PL. Under the condition of near-resonant excitation when the interference of smaller QDs is inhibited, sample 2 (with closely lying dots) displays a peculiar behavior highlighted in Fig. 4(e). A bow appears at a distance of one LO-phonon energy from the PL maximum. In Fig. 4(f) we show the calculated value of the decay time renormalization by phonon emission¹⁰ given the QD size distribution that follows the shape of the PL emission spectrum reinforcing the role of phonons in the process of carrier transfer.

III. CONCLUDING REMARKS

The characterization of carrier dynamics detected by time resolved PL can be a complex task since various processes compete and can appear as simultaneous effects. We have evaluated the role of optical phonons in the reduction of the

decay time in coupled QDs as those present in QD chains. Also influenced by the asymmetric carrier transfer assisted by phonon emission, nonlinear contributions to the PL dynamics appear due to relative charge imbalance. It leads to an increase of the decay time as the emission energy approaches the PL maximum and provokes a nonmonotonic behavior. Such a behavior has been obtained systematically in different QD samples of different composition. For electronically uncoupled QDs, a monotonic behavior is expected if the charging conditions of all the dots are un-correlated. However, in this case, the optical coupling⁶⁻⁸ may affect the value of the decay time when the appearance of super-radiant or

subradiant modes becomes the leading effect. We believe that this discussion contributes with additional ingredients to the rich phenomenology involved in the process of optical recombination in QDs.

ACKNOWLEDGMENTS

We thank L. Worschech, Technische Physik, Physikalisches Institut, Universität Würzburg, for motivating discussions. The authors acknowledge the financial support of the Brazilian agencies CAPES, CNPQ, and FAPESP. V.G.D., G.J.S., and Yu.I.M. acknowledge the support of NSF Grant No. DMR-0520550.

*dfcesar@df.ufscar.br

¹U. Bockelmann, *Phys. Rev. B* **48**, R17637 (1993).

²Weidong Yang, Roger R. Lowe-Webb, Hao Lee, and Peter C. Sercel, *Phys. Rev. B* **56**, 13314 (1997).

³M. Paillard, X. Marie, E. Vanelle, T. Amand, V. K. Kalevich, A. R. Kovsh, A. E. Zhukov, and V. M. Ustinov, *Appl. Phys. Lett.* **76**, 76 (2000).

⁴J. W. Tomm, T. Elsaesser, Yu. I. Mazur, H. Kissel, G. G. Tarasov, Z. Ya. Zhuchenko, and W. T. Masselink, *Phys. Rev. B* **67**, 045326 (2003).

⁵B. R. Wang, B. Q. Sun, Y. Ji, X. M. Dou, Z. Y. Xu, Zh. M. Wang, and G. J. Salamo, *Appl. Phys. Lett.* **93**, 011107 (2008).

⁶M. Scheibner, T. Schmidt, L. Worschech, A. Forchel, G. Bacher, T. Passow, and D. Hommel, *Nat. Phys.* **3**, 106 (2007).

⁷Yu. I. Mazur, V. G. Dorogan, E. Marega Jr., G. G. Tarasov, D. F. Cesar, V. Lopez-Richard, G. E. Marques, and G. J. Salamo, *Appl. Phys. Lett.* **94**, 123112 (2009).

⁸Yu. I. Mazur, V. G. Dorogan, E. Marega Jr., D. F. Cesar, V. Lopez-Richard, G. E. Marques, Z. Ya. Zhuchenko, G. G. Tarasov, and G. J. Salamo, *Nanoscale Res. Lett.* **5**, 991 (2010).

⁹E. Margapoti, L. Worschech, S. Mahapatra, K. Brunner, A. Forchel, Fabrizio M. Alves, V. Lopez-Richard, G. E. Marques, and C. Bougerol, *Phys. Rev. B* **77**, 073308 (2008).

¹⁰V. Lopez-Richard, S. S. Oliveira, and G.-Q. Hai, *Phys. Rev. B* **71**, 075329 (2005).

¹¹P. M. Lytvyn, Yu. I. Mazur, E. Marega Jr., V. G. Dorogan, V. P. Kladko, M. V. Slobodian, V. V. Strelchuk, M. L. Hussein, M. E. Ware, and G. J. Salamo, *Nanotechnology* **19**, 505605 (2008).

¹²A. Tackeuchi, Y. Nakata, S. Muto, Y. Sugiyama, T. Usuki, Y. Nishikama, N. Yokoyama, and O. Wada, *Jpn. J. Appl. Phys.* **34**, L1439 (1995).

¹³S. Malik, E. C. Le Ru, D. Childs, and R. Murray, *Phys. Rev. B* **63**, 155313 (2001).

¹⁴L. Villegas-Lelovsky, M. D. Teodoro, V. Lopez-Richard, C. Calseverino, A. Malachias, E. Marega Jr., B. L. Liang, Yu. I. Mazur, G. E. Marques, C. Trallero-Giner, and G. J. Salamo, *Nanoscale Res. Lett.* **6**, 56 (2011).

¹⁵E. Margapoti, Fabrizio M. Alves, S. Mahapatra, T. Schmith, V. Lopez-Richard, C. Destefani, E. Menendez-Proupin, Fanyao Qu, C. Bougerol, K. Brunner, A. Forchel, G. E. Marques, and L. Worschech, *Phys. Rev. B* **82**, 205318 (2010).

¹⁶A. Debernardi, *Phys. Rev. B* **57**, 12847 (1998).

¹⁷L. Jacak, J. Krasnyj, and W. Jacak, *Phys. Lett. A* **304**, 168 (2002).

¹⁸Yu. I. Mazur, V. G. Dorogan, E. Marega Jr., P. M. Lytvyn, Z. Ya. Zhuchenko, G. G. Tarasov, and G. J. Salamo, *New J. Phys.* **11**, 043022 (2009).

¹⁹W. Shockley and W. T. Read Jr., *Phys. Rev.* **87**, 835 (1952).